

Geochronology Beyond Radiocarbon: Optically Stimulated Luminescence Dating of Palaeoenvironments and Archaeological Sites

Constantin D. Athanassas¹ and Günther A. Wagner²

1811-5209/16/0012-0027\$2.50 DOI: 10.2113/gselements.12.1.27

This article reviews optically stimulated luminescence (OSL) dating as used on Quaternary sediments and for archaeological dating. The underlying physics is summarized and the laboratory method itself is described. Examples of OSL dating illustrate its use in palaeoenvironmental and archaeological contexts, although problems associated with the technique are also addressed. Finally, we discuss long-range variants of OSL that may help date deposits currently considered too old for OSL to be applied.

KEYWORDS: long-range luminescence dating, sediments, Quaternary geology, anthropogenic deposits

INTRODUCTION

The last few decades have seen a significant impact of geoscience techniques and concepts on palaeoenvironmental and (geo)archaeological studies. Geoarchaeology and palaeoenvironmental studies both require a solid chronological framework by which to recognize causes and effects, as well as rates of processes. For this purpose, in addition to archaeological and geomorphological reasoning, radiocarbon dating (¹⁴C) is used to date organic materials. But in view of its ineffectiveness to date materials older than 50 ka and the omnipresence of (inorganic) clastic sediments in most depositional contexts, optically stimulated luminescence (OSL) dating and its long-range dating alternatives are indispensable.

Optically stimulated luminescence was pioneered in the 1980s by Huntley et al. (1985) as the successor to thermoluminescence (TL). Rapid signal resetting of OSL under direct or indirect sunlight (bleaching) rendered OSL pivotal in sediment dating because it can date the time elapsed since the last exposure of natural minerals to daylight. It soon became evident that OSL could be applicable to dating numerous types of sedimentary environments—aeolian, coastal, fluvial, glacial, and lacustrine—thereby enhancing our understanding of Earth's surface processes (Rhodes 2011; Roberts et al. 2015) and of human evolution (Jacobs et al. 2008; Wagner et al. 2010).

Recent luminescence methods are collectively known as long-range dating variants, and these include thermally transferred optically stimulated luminescence (TT-OSL), post-infrared infrared stimulated luminescence (pIR-IRSL), multi-elevated temperature post-infrared infrared stimulated

luminescence (MET-pIR-IRSL), violet stimulated luminescence (VSL), and infrared-radiofluorescence (IR-RF). These new methods have allowed chronometric dating on sedimentary deposits that goes beyond the usual distal age limit of conventional OSL dating, which is estimated to be about 200,000 years (Rhodes 2011; Roberts et al. 2015).

This paper aims to inform geoscientists, archaeologists, and geoarchaeologists about the physical

background, methodology, and applications of optically stimulated luminescence dating. The case studies illustrated here are mainly drawn from the authors' own work and provide applications of OSL dating and its long-range variants to best advantage, as well as giving examples that challenge their performance.

FUNDAMENTALS OF OSL DATING: TECHNIQUES AND LIMITING FACTORS

Dating by optically stimulated luminescence builds on the phenomenon that light is emitted from ionized geological minerals when undergoing optical stimulation. Natural ionizing radiation is universal and includes radioactivity—expressed by the emission of α , β , and γ rays from decaying atomic nuclei of ²³⁵U, ²³⁸U, ²³²Th, and ⁴⁰K—and cosmic rays. Natural ionizing radiation excites the mineral to a prolonged excitation state in which electrons accumulate in lattice defects inherent to the mineral; the longer the ionization over geological time the larger the amount of trapped charge.

An OSL age is the ratio of the radiation dose to the rate at which it was absorbed. Sophisticated instruments known as “luminescence readers” can reset excited minerals to the ground state by stimulating them with artificial light and recording their luminescence. Among natural minerals, quartz and feldspar are the most suitable geochronometers to date by OSL: their luminescence is typically stimulated with blue (470 nm) and infrared (870 nm) light, respectively. In the case of feldspar, released luminescence is termed infrared stimulated luminescence (IRSL). However, feldspars frequently undergo loss of trapped electrons at ambient temperatures, a phenomenon known as anomalous fading (Wintle 1973), which, if not corrected, can result in severe age underestimation.

Luminescence intensity tails off with stimulation time and can be graphically represented by a decay curve (Figs. 1A, B). Luminescence intensity is more or less proportional to the dose. The laboratory equivalent of the natural dose, known as the equivalent dose (D_e), the SI unit for

1 Centre de Recherche & d'Enseignement de Géosciences de l'Environnement CEREGE, Europôle Méditerranéen de l'Arbois, Aix-en-Provence, France
E-mail: athanassas@cerege.fr

2 Geographisches Institut der Universität Heidelberg, Germany
E-mail: gawag-wagner@web.de

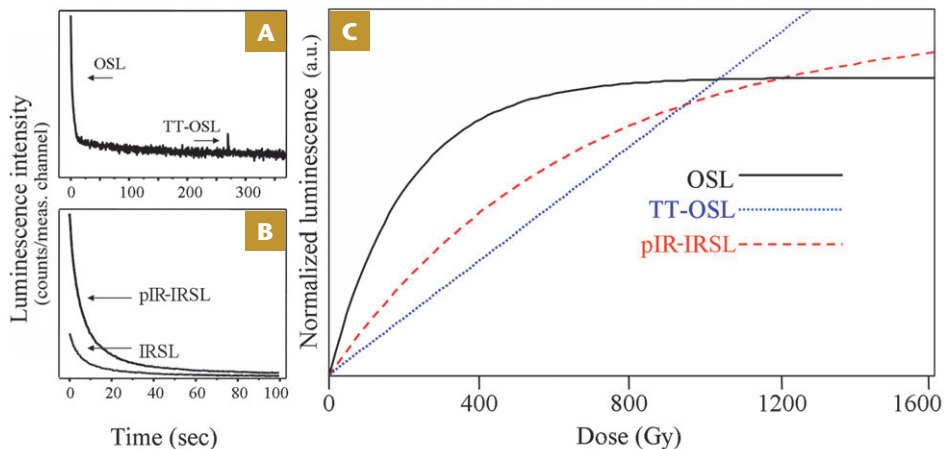


FIGURE 1 (A) Signals (decay curves) from optically stimulated luminescence (OSL) and thermally transferred optically stimulated luminescence (TT-OSL) of quartz. (B) Signals (decay curves) from infrared stimulated luminescence (IRSL) and post-infrared infrared stimulated luminescence (pIR-IRSL) of feldspar. (C) The corresponding growth curves for quartz (OSL, TT-OSL) and feldspar (pIR-IRSL). Dose is in grays (Gy), and units of luminescence intensity are in counts per measurement channel.

which is the gray (symbol Gy; $\text{Gy} = \text{J}\cdot\text{kg}^{-1}$). The D_e can be evaluated by interpolating the natural OSL signal intensity into a formula, either linear or exponential, that represents the best fit to an empirical plot containing pairs of known doses (regenerated doses) with their associated OSL signal intensities. Thermal treatments are interposed each time a dose is administered to remove electrons from geologically unstable crystal defects. Heating may induce changes to the luminescence efficiency (sensitivity) of the crystal, which should be monitored and corrected. Thus, natural and regenerated signals are normalized against that of a fixed dose (test dose). The resulting plot is termed a “growth curve” (FIG. 1C)

The above method of D_e evaluation is known as the single aliquot regenerated (SAR) dose protocol (Galbraith et al. 1999; Murray and Wintle 2000). The single aliquot regenerated dose protocol for the measurement of D_e has the advantage of enabling replicate measurements (TABLE 1) on individual subsamples (aliquots), which facilitates recording the fluctuations in D_e for the sample.

Estimation of the dose rate involves determining radioelement concentrations either by standard analytical methods, such as neutron activation analysis (NAA) or inductively coupled plasma mass spectrometry (ICPMS), or techniques based on the emission of α , β , and γ rays from the decaying nuclei, such as alpha- and beta-particle counting, or gamma spectroscopy. Radioelement concentrations are then converted to dose-rate units ($\text{Gy}\cdot\text{ka}^{-1}$) using conversion factors (Guérin et al. 2011) that deliver the dose rate per radioelement’s concentration (ppm). The dose rate can also be measured in situ by placing dosimeters in locations from where samples were taken. The dosim-

eters are $\text{Al}_2\text{O}_3\text{:C}$ crystal pellets with exceptional sensitivity to natural ionizing radiation. Dosimeters are usually in place for several months to register the total dose rate contributed from all local potential inputs. Specifically, in situ measurements of gamma dose rate can be accelerated by employing field gamma spectrometers that incorporate sodium iodide (NaI) crystal detectors. The acquired spectrum, resulting from the gamma ray emission of U, Th, and K, can then be converted to a dose rate.

Parallel to sediment dating, OSL is also capable of dating the numerical age of architectural remains (Liritzis 2011). This can be done by estimating the time elapsed since the last exposure of a stone’s surface to sunlight. Optically stimulated luminescence dating of ancient architecture is grounded on the assumption that stone surfaces (e.g. masonry, slabs, orthostats, and pillars) would receive sufficient daylight before they were assembled together to erect the structure. If an adequate amount of quartz grains can be extracted, which would involve only sampling the surface of the stone, then conventional OSL dating protocols could be employed to generate a numerical age for the structure.

Precision in OSL dating is a serious concern user. The degree of tolerance to precision is case-specific but, usually, anything less than 10% is satisfactory. Several factors may serve as sources of error. These include intrinsic ones related to the crystalline properties of the material, or extrinsic ones due to factors such as differential bleaching or post-depositional sediment mixing. Aliquots composed of multiple grains with different bleaching and burial histories can have an undesirable impact on the precision of the average D_e . However, such uncertainties do

TABLE 1 SUMMARY OF SINGLE ALIQUOT REGENERATED DOSE PROTOCOLS FOR OSL, TT-OSL AND pIR-IRSL (MEASURED AT 290°C) DATING. Measurement settings are default values by Murray and Wintle (2000) for OSL, Stevens et al. (2009) for TT-OSL, and Thiel et al. (2011) for pIR-IRSL.

Treatment	OSL	TT-OSL	pIR-IRSL	Result
Mineral	quartz	quartz	feldspar	—
Dose	variable	variable	variable	Replenish charge (no irradiation before measurement of the natural signal)
Preheat	220°C	260°C	260°C	Remove thermally unstable trapped charge
Stimulation	470 nm @ 125°C	470 nm @ 125°C	870 nm @ 50°C	Record of primary signal
Preheat	—	260°C	—	Access thermally stable charge
Stimulation	—	470 nm @ 125°C	870 nm @ 290°C	Record secondary signal (TT-OSL, pIRIR)
Test dose	fixed value	fixed value	fixed value	Replenish charge
Preheat	220°C	260°C	260°C	Remove thermally unstable trapped charge
Stimulation	470 nm @ 125°C	470 nm @ 125°C	870 nm @ 50°C	Normalization of primary signals
Preheat	—	260°C	—	Access thermally stable charge
Stimulation	—	470 nm @ 125°C	870 nm @ 290°C	Normalization of secondary signals (TT-OSL, pIRIR)

not apply to grains measured individually. For this reason, OSL geochronologists often turn to single grains to achieve greater resolution (Duller et al. 2015; Roberts et al. 2015). Age models constitute a statistical means of recognizing clusters of grains with distinct exposure/burial histories within a sample (Galbraith et al. 1999), which enables the most representative age for a depositional event to be determined.

While ages as young as a few decades can be estimated, the oldest age limit of OSL dating is controlled by the saturation of luminescence (i.e. limited response to the increasing dose). The rate at which luminescence becomes saturated is defined by the local dose rate: this restricts OSL dating in typical sedimentary environments to less than ~200,000 years (Rhodes 2011; Arnold et al. 2014; Roberts et al. 2015). Novel variants of luminescence dating can surpass that maximum, pushing its performance limits deeper into the Pleistocene.

LONG-RANGE OSL DATING METHODS

Long-range OSL dating methods have been invented for both quartz and feldspar. These methods take advantage of latent signals than manifest themselves under thermal treatment of the minerals involved.

Thermally transferred OSL (TT-OSL) is an underlying signal accessed during thermal treatment of quartz (pre-heat) after having erased the natural OSL signal (TABLE 1). Thermally transferred OSL is characterized by having substantially higher saturation levels than conventional OSL (Wang et al. 2007). For samples rich in quartz, which have experienced typical environmental dose rates (~1 Gy·ka⁻¹), single aliquot regenerated based TT-OSL protocols can theoretically make precise age determinations back to the Early Pleistocene (Athanasas and Zacharias 2010), a prediction later verified by Pickering et al. (2013) of palaeoanthropologically significant caves in South Africa.

Violet stimulated luminescence (VSL) refers to the emission of ultraviolet luminescence during the stimulation of quartz by photons from the violet part of the spectrum (405 nm). Violet stimulated luminescence lacks the intensity of typical OSL and, for this reason, the sample must undergo illumination by blue light prior to the violet stimulation (Jain 2009) so that the VSL is detectable. Ankjærgaard et al. (2013) asserted that the growth of VSL can go as high as ~6,400 Gy, which would extend the typical maximum limit of OSL dating by 20 times and so allow dating over the entire Middle Pleistocene.

With respect to feldspar, the post-infrared infrared stimulated luminescence (pIR-IRSL) retains all the known advantages of feldspar over quartz (i.e. intense signals under laboratory stimulation and considerably higher saturation levels) while additionally tackling the issue of anomalous fading. A pIR-IRSL procedure based on the SAR model is grounded on the fact that as IR stimulation of feldspars is carried out at progressively higher temperatures so the generated infrared stimulated luminescence (IRSL) signals are characterized by progressively lower fading rates, resulting in more accurate D_e estimates. A SAR-based method for pIR-IRSL (Thiel et al. 2011) (TABLE 1) has established pIR-IRSL as a means by which to date the Middle Pleistocene sedimentary rock record (Arnold et al. 2014; Roberts et al. 2015).

Li and Li (2011) put forward an alternative pIR-IRSL method for that eliminated the necessity of correcting for anomalous fading by measuring the pIR-IRSL signal at multielevated temperatures (MET) until a plateau of signals unaffected by fading is reached (usually at >200 °C). This

MET-pIR-IRSL technique has dated samples as old as at least 300 ka (Roberts et al. 2015) and made it possible for MET-pIR-IRSL to date the entire Middle Pleistocene (Roberts et al. 2015).

However, the effectiveness of high-temperature pIR-IRSL signals in enhancing Quaternary geochronology may go amiss if prolonged predepositional bleaching cannot be made certain: pIR-IRSL signals are reset more slowly than IRSL (50 °C) and quartz-OSL.

Alkali-feldspars have the potential for extending age ranges by making use of their radiofluorescence (RF) properties. Radiofluorescence in alkali-feldspars is emitted in the infrared (IR) region (865 nm) of the spectrum and results from electron transitions in the crystal induced by ionizing radiation. One use of IR-RF was in deciphering the chronology of *Homo heidelbergensis* in Europe (Wagner et al. 2010).

CASE STUDIES

Dating Palaeogeography

Athanasas et al. (2012) combined OSL and TT-OSL dating to work out a chronological outline for Upper Palaeolithic hominin activity and coastal palaeogeographic changes at Navarino on the Ionian Sea (southwest Peloponnese, Greece). Dating by OSL of archaeological layers that contain assemblages of Upper Palaeolithic chipped stone artifacts bracketed the chronology of hominin activity at Navarino between oxygen isotope stage 5 (OIS-5 at ~120 ka) and oxygen isotope stage 2 (OIS-2 at ~20 ka). Having established a chronological framework for the Mousterian (Neanderthal) layers, Athanasas et al. (2012) went further by correlating the OSL chronology with known Late Pleistocene sea-level stands, enabling a reconstruction of the regional palaeogeography.

Athanasas et al. (2012) demonstrated that the location of the Palaeolithic sites relative to the coast was framed by two palaeogeographic extremes developed during the Last Interglacial (LI = OIS-5) and the Last Glacial Maximum (LGM = OIS-2), respectively. The overall sea-level drop following the LI kept segments of the Ionian shelf exposed until the LGM. Palaeolithic exploitation strategies would, therefore, have been affected by the shifting coastal geomorphology, compelling Upper Palaeolithic hominins to acclimatize to new environmental conditions.

Dating Peridesert Loess

The Canary Islands are located off the west coast of Africa in the Atlantic Ocean (FIG. 2) and are affected by the ecoclimatic zones of West Africa, namely the Saharan and the Sahelian. The Canary Islands experience dusty winds from the east that derive from the Sahara Desert on a seasonal basis (FIG. 2A). Saharan dust fallout is an important factor in soil development on the Canary Islands (Menéndez et al. 2009).

Terrestrial sedimentary sequences from the Canary Islands are rich in Saharan dust; therefore, they can be used as proxies for the palaeoenvironmental evolution of the Sahara Desert (von Suchodoletz et al. 2010). Although the desertification history of northwest Africa is well documented for the Holocene and the Late Pleistocene (Petit-Maire et al. 1994), it is only intermittently known from the terrestrial records of the Middle and Early Pleistocene (von Suchodoletz et al. 2010). Fortunately, a well-preserved and continuous terrestrial record of “missing-links” from the north-African desertification history exists in the Canary

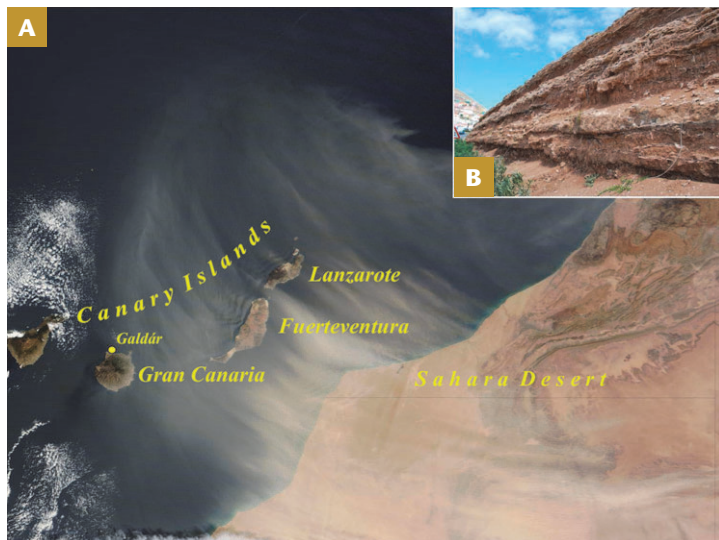


FIGURE 2 (A) Saharan dust storm over the Canary Islands in March 2012. NASA IMAGE COURTESY JEFF SCHMALTZ, LANCE/ EOSDIS MODIS RAPID RESPONSE TEAM AT NASA GSFC. (B) Sequence of loessoid at Galdár, Gran Canaria.

Islands, which not only captures the latest parts of the Quaternary but also extends further back to the Pleistocene (Menéndez et al. 2009).

Occurrences of desert loess have been dated using OSL in the easternmost islands of Fuerteventura and Lanzarote (von Suchodoletz et al. 2010). And a strong airborne-dust component rich in quartz has been found in silted-up catchments on Gran Canaria (Menéndez et al. 2009). Because quartz is exotic to the Canary Islands (whose geology is almost all mafic volcanics) its abundance in palaeosols and loess-like deposits (loessoids) signals a Saharan provenance, evoking important chronological and palaeoclimatic implications.

Inspired by the preceding dating studies on the eastern Canary islands (von Suchodoletz et al. 2010), Athanassas embarked on a mission to the Canary Islands to do research using OSL to define the chronology of loess deposits on Gran Canaria. A representative loessoid outcrop in Galdár was identified and sampled (FIG. 2B). The term “loessoid” designates peri-Saharan dust amassed at rates lower than typical loesses (Menéndez et al. 2009). A Middle to Late Pleistocene age had been speculated for this loessoid on the basis of geomorphology and modern dust accumulation rates on Gran Canaria (Menéndez et al. 2009).

Equivalent doses of Saharan quartz from the Galdár deposit were estimated using the standard SAR procedure for quartz by Murray and Wintle (2000). When the SAR dose-estimates were divided with the local dose rate, they returned a Late-Middle Pleistocene age (0.18 Ma) for Saharan dust deposition on northern Gran Canaria (TABLE 2).

This OSL age is consistent with the beginning of a chronological interval in the palaeoenvironmental history of the Canary Islands during which regional moisture underwent fluctuations between glacial and interglacial periods (von Suchodoletz et al. 2010). Specifically, modulations to the regional atmospheric circulation pattern during glacial stages forced antitrade winds (prevailing winds from the west to the east in mid latitudes) to shift southwards, allowing these anti-trade winds to convey their moisture over areas of North Africa (von Suchodoletz et al. 2010). An additional input of moisture into the mid-Pleistocene regional hydrological systems might relate to the African

summer monsoon, brief spells of which affected the archipelago during the same period of time (von Suchodoletz et al. 2010).

Dating Soil Erosion

The basin of Phlious on the northern Peloponnese (Greece) has been populated since the Early Neolithic period. When the early farmers cleared the forests, the freshly exposed surface became vulnerable to soil erosion, in particular on the gentle slopes around the basin.

The soil material was washed downwards by the precipitation and was deposited as colluvium at the foot-slope. This process continued as long as agricultural activities went on. Therefore, by dating these sediments one can gain insights into changes of human land use and/or of climatic conditions at the time of their deposition. With OSL one can date the colluvial deposition directly, provided the feldspar and quartz grains were sufficiently bleached during their down-slope transport.

Quartz OSL ages indicate that colluvia were being deposited since the Early Neolithic (7th millennium BC). The age distribution allows calculation of sedimentation rates, which indicate the various cultural periods when land use was intensified (FIG. 3). The sedimentation rate was very low during the pre-Neolithic, but clearly increased at the beginning of the Neolithic. During the Chalcolithic and the Early Bronze Age, it was low again, but increased once more during the Middle and Late Bronze Age (Fuchs et al. 2004). Analogous patterns of colluvial formation since the Neolithic have also been observed at several sites in southwestern Germany (Lang et al. 1999). In all these cases, the alternating rates of sedimentation seem to correlate with cultural and population development.

Dating Coastal Plain Evolution

Theodorakopoulou et al. (2012) investigated the coasts of northeastern Crete and found that the coastal plains that bound the Gulf of Mirabello had been influenced by Holocene climatic events. Their multidisciplinary effort – synthesizing quartz-OSL dating and ¹⁴C dating of alluvial sediment cores, and micropalaeontological analysis – established a Holocene age for most of the coastal plain. Their research also demonstrated how well-documented climatic events affected the development of the alluvial plain and deteriorated archaeological settlement patterns.

Major defining points of Holocene climatic history were recognized within the local sedimentary record via abrupt changes in the sedimentation rate. Two well-separated events of substantial sediment accumulation were dated by OSL and ¹⁴C to around the Holocene Thermal Optimum at ~8–4 ka BP (before present) and the Roman Climatic Optimum at ~2.2–1.5 ka BP. Those events were each succeeded by episodes of no alluvial deposition, which can be correlated to dry-to-cool periods at ~4 ka BP and the Dark Ages Cold Period at ~1.5–1.1 ka BP, respectively. Of all of these episodes, the resurgence of sedimentation during the Roman Climatic Optimum seemed to have had a tremendous impact on the settlement pattern in the form of flash-flooding events, as deduced from sediment cores (Theodorakopoulou et al. 2012). This evidently diminished human habitation on the coastal plain.

Dating Geomagnetic Reversals

The Central Mediterranean exhibits archetypical Quaternary marine sequences, many of which are regarded as global stratotypes for the Early and Middle Pleistocene (Papanikolaou et al. 2011). On the island of Zante (or Zakynthos), in the Ionian Sea, there is an uplifted marine

sequence that has been studied by Papanikolaou et al. (2011). These authors used magnetostratigraphy to produce a chronostratigraphic framework for the uplifted sequence (Fig. 4), which captures the last geomagnetic reversal, known as the Brunhes/Matuyama boundary (0.77 Ma), and a subsequent geomagnetic excursion known as “17a” (0.66 Ma).

With the goal of assessing the age-range that can be attained by elevated-temperature IRSL dating methods, Athanassas tested sediments from the Zante marine sequence using the dating protocol of Thiel et al. (2011) against the well-defined magnetostratigraphy of the reference sequence. So far, only a few ages over 300 ka and only a single one over 600 ka have been reported (Arnold et al. 2014; Roberts et al. 2015 and references therein). Therefore, the Zante sequence poses a challenge to the methodology tested. The protocol used by Thiel et al. (2011) measures pIR-IRSL from feldspar at 290°C (pIRIR₂₉₀), after having erased conventional IRSL at 50°C (TABLE 1). This method was tested on sediments from the Brunhes/Matuyama boundary and the 17a geomagnetic excursion (Fig. 4).

The calculation of accurate pIRIR₂₉₀ ages is complicated by the difficulty in generating reliable equivalent doses over all of the sequence: equivalent doses appeared to be broadly spread (TABLE 2). It is known that post-infrared IRSL can experience residual doses that cannot be totally removed (Arnold et al. 2014). Intersample variations in hard-to-bleach large residual doses might explain the scatter seen here. Despite this, two samples with fading-corrected equivalent doses brought forth ages that coincide with the Brunhes/Matuyama (B/M) and 17a events at 0.72 ± 0.14 Ma and 0.62 ± 0.18 Ma, respectively (TABLE 2). This suggests that if low residual doses can be ensured, then pIR-IRSL can be exceptionally successful.

CONCLUSIONS

Palaeoenvironments influence major human evolutionary and cultural shifts. Optically stimulated luminescence (OSL) dating can link major environmental events with human cultural changes on timescales greater than ¹⁴C dating can manage. Sharp signal resetting in most sunlit environments has established OSL as the dominant technique in dating sedimentary deposits associated with

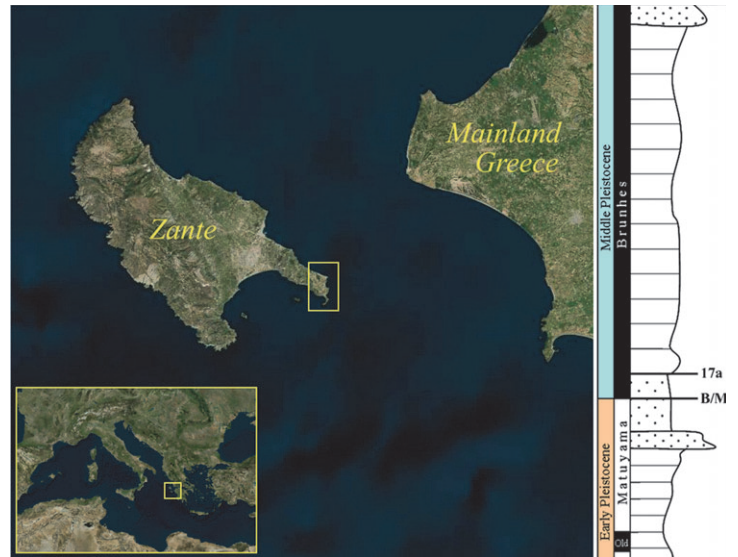


FIGURE 4 (LEFT) Satellite images showing the location of the Quaternary marine sequence studied by high-temperature post-infrared infrared stimulated luminescence (pIR-IRSL). The sequence location (indicated by the yellow box on southeast Zante Island) is in the central Mediterranean off the coast of mainland Greece. (RIGHT) A simplified illustration of the Early–Middle Pleistocene stratigraphy for this marine sequence. The Brunhes–Matuyama boundary (B/M) and subsequent geomagnetic excursion known as “17a” are indicated. SATELLITE IMAGES © HARRIS CORP, EARTHSTAR GEOGRAPHICS LLC, SIO, © 2015 MICROSOFT CORPORATION.

the Earth’s surface and with anthropogenic processes during the last glacial–interglacial cycle. Even though the dose rate may confine conventional OSL dating to the Late Quaternary, novel OSL variants that make use of latent luminescence signals and that exhibit higher saturation levels can surpass that conventional boundary. Long-range OSL dating variants are continually being put to the test, and they continue to demonstrate their adaptability to different settings and periods of geological time. These long-range OSL techniques are enhancing the study of human evolution and landscapes in which they (hominins) lived, allowing us to peer deeper into the Pleistocene.

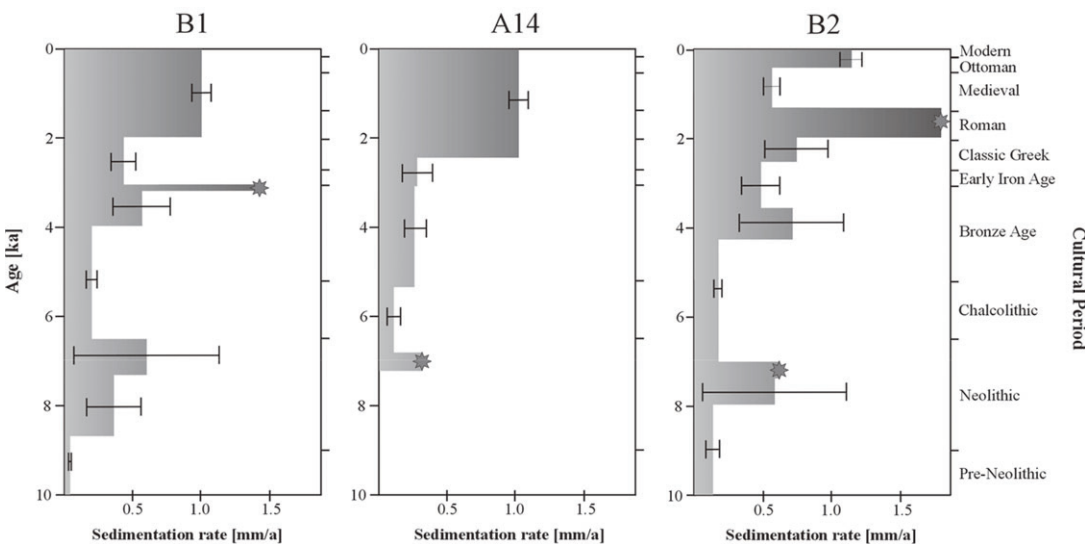


FIGURE 3 Sedimentation rates of colluvia for various archaeological periods of the Phlious basin (northeast Peloponnese, Greece) determined by OSL from quartz. The error bars represent the uncertainty on the sedimentation rate estimates. The star on each graph represents minimum sedimentation rates,

with true values being higher. Samples B1, A14, and B2 correspond to different study sites, and the differences between their corresponding plots indicate different sedimentation patterns. AFTER FUCHS ET AL. (2004).

TABLE 2 Indicative radioelement concentrations, dose rates, equivalent doses (D_e) and OSL ages for the loessoid deposit at Galdár, Gran Canaria and the marine sequence on Zante. Zante 1–4 represent samples from the Bruhnes/Matuyama (B/M) boundary and 17a excursion. N.A. = not applicable.

Origin	Sample	Geomagnetic event	Magneto-stratigraphic age (Ma)	U (ppm)	Th (ppm)	K (wt%)	Dose rate ($Gy\ ka^{-1}$)	D_e (Gy)	Age (Ma)
Canary Islands	Galdár loess	N.A.	N.A.	2.9 ± 0.1	9.3 ± 0.1	1.05 ± 0.01	2.98 ± 0.20	524 ± 53	0.18 ± 0.02
Greece	Zante1	B/M reversal	0.77	1.5 ± 0.1	4.7 ± 0.1	0.95 ± 0.01	1.56 ± 0.	1126 ± 229	0.72 ± 0.14
Greece	Zante2	17a excursion	0.66	1.1 ± 0.1	1.6 ± 0.1	0.16 ± 0.01	0.64 ± 0.01	716 ± 87	1.12 ± 0.14
Greece	Zante3	17a excursion	0.66	1.8 ± 0.1	1.9 ± 0.1	0.3 ± 0.01	0.95 ± 0.01	875 ± 180	0.92 ± 0.19
Greece	Zante4	17a excursion	0.66	2.5 ± 0.1	4.6 ± 0.1	0.99 ± 0.01	1.96 ± 0.01	1224 ± 168	0.62 ± 0.18

ACKNOWLEDGMENTS

The study by OSL of sediments from the Canary Islands was supported by an ESF-MedCLIVAR grant awarded to CDA in 2011. CDA was hosted by the Departamento de Física Universidad de Las Palmas de Gran Canaria (ULPGC) and he is thankful to Francisco José Pérez Torrado (GeoVol, ULPGC), Inmaculada Menéndez González (IOCAG, ULPGC) and Juan Francisco Betancor Lozano (Laboratorio de Palaeontología, ULPGC). Sampling of the marine

sequence on Zante Island was guided by M. Papanikolaou (Ichron Ltd, UK). Material from the Canary Islands and Zante was measured by CDA at the OSL laboratory of NCSR DEMOKRITOS, Athens (Greece) during the period 2011–2012. We are thankful to RG Roberts (University of Wollongong, Australia) for his valuable comments on the manuscript. Radioelement concentrations were measured by ICPMS at Acme Analytical Laboratories in Vancouver (Canada). ■

REFERENCES

- Ankjærgaard C, Jain M, Wallinga J (2013) Towards dating Quaternary sediments using the quartz violet stimulated luminescence (VSL) signal. *Quaternary Geochronology* 18: 99–109
- Arnold LJ and 6 coauthors (2014) Evaluating the suitability of extended-range luminescence dating techniques over early and Middle Pleistocene timescales: Published datasets and case studies from Atapuerca, Spain. *Quaternary International*, doi: 10.1016/j.quaint.2014.08.010
- Athanassas C, Bassiakos Y, Wagner GA, Timpson ME, (2012) Exploring palaeogeographic conditions at two palaeolithic sites in Navarino, southwest Greece, dated by optically stimulated luminescence. *Geoarchaeology* 27: 237–258
- Athanassas C, Zacharias N (2010) Recuperated-OSL dating of quartz from Aegean (South Greece) raised Pleistocene marine sediments: current results. *Quaternary Geochronology* 5: 65–75
- Duller GAT, Tooth S, Barham L, Tsukamoto S (2015) New investigations at Kalambo Falls, Zambia: Luminescence chronology, site formation, and archaeological significance. *Journal of Human Evolution* 85: 111–125
- Fuchs M, Lang A, Wagner GA (2004) The history of Holocene soil erosion in the Phlious basin, NE Peloponnese, Greece, based on optical dating. *The Holocene* 14: 334–345
- Galbraith RF, Roberts RG, Laslett GM, Yoshida H, Olley JM (1999) Optical dating of single and multiple grains of quartz from Jinmium rock shelter, northern Australia: Part I, Experimental design and statistical models. *Archaeometry* 41: 339–364
- Guérin G, Mercier N, Adamiec G (2011) Dose rate conversion factors: update. *Ancient TL* 29: 5–8
- Huntley DJ, Godfrey-Smith DI, Thewalt MLW (1985) Optical dating of sediments. *Nature* 313: 105–107
- Jacobs Z and 8 coauthors (2008) Ages for the Middle Stone Age of southern Africa: implications for human behavior and dispersal. *Science* 322: 733–735
- Jain M (2009) Extending the dose range: probing deep traps in quartz with 3.06 eV photons. *Radiation Measurements* 44: 445–452
- Lang A, Kadereit K, Behrends RB, Wagner GA (1999) Optical dating of anthropogenic sediments at the archaeological excavation site Herrenbrunnenbuckel, Bretten-Bauerbach, Germany. *Archaeometry* 41: 397–411
- Li B, Li S-H (2011) Luminescence dating of K-feldspar from sediments: a protocol without anomalous fading correction. *Quaternary Geochronology* 6: 468–479
- Liritzis I (2011) Surface dating by luminescence: an overview. *Geochronometria* 38: 292–302
- Menéndez I, Cabrera L, Sánchez-Páez I, Mangas J, Alonso I (2009) Characterisation of two fluvio-lacustrine loessoid deposits on the island of Gran Canaria, Canary Islands. *Quaternary International* 196: 36–43
- Murray AS, Wintle AG (2000). Luminescence dating of quartz using an improved single-aliquot regenerative-dose protocol. *Radiation Measurements* 32: 57–73
- Papanikolaou MD and 5 coauthors (2011) A well-established Early–Middle Pleistocene marine sequence on southeast Zakynthos island, western Greece: Magneto-biostratigraphic constraints and palaeoclimatic implications. *Journal of Quaternary Science* 26: 523–540
- Petit-Maire N, Reyss J-L, Fabre J (1994) Un paléolac du dernier interglaciaire dans une zone hyperaride du Sahara Malien (23°N). *Comptes Rendus de l'Académie des Sciences, série II* 319: 805–809
- Pickering R and 8 coauthors (2013) Palaeoanthropologically significant South African sea caves dated to 1.1–1.0 million years using a combination of U–Pb, TT-OSL and palaeomagnetism. *Quaternary Science Reviews* 65: 39–52
- Rhodes EJ (2011) Optically stimulated luminescence dating of sediments over the past 200,000 Years. *Annual Review of Earth and Planetary Sciences* 39: 461–488
- Roberts RG and 5 coauthors (2015) Optical dating in archaeology: thirty years in retrospect and grand challenges for the future. *Journal of Archaeological Science* 56: 41–60
- Stevens T, Buylaert J-P, Murray AS (2009) Towards development of a broadly-applicable SAR TT-OSL dating protocol for quartz. *Radiation Measurements* 44: 639–645
- Theodorakopoulou K, Pavlopoulos K, Athanassas C, Zacharias N, Bassiakos Y (2012) Sedimentological response to Holocene climate events in the Istron area, Gulf of Mirabello, NE Crete. *Quaternary International* 266: 62–73
- Thiel C and 6 coauthors (2011) Luminescence dating of the Stratzing loess profile (Austria) – Testing the potential of an elevated temperature post-IR IRSL protocol. *Quaternary International* 234: 23–31
- Von Suchodoletz H and 5 coauthors (2010) Soil moisture fluctuations recorded in Saharan dust deposits on Lanzarote (Canary Islands) over the last 180 ka. *Quaternary Science Reviews*, doi: 10.1016/j.quascirev.2010.05.014
- Wagner GA and 9 coauthors (2010) Radiometric dating of the type-site for *Homo heidelbergensis* at Mauer, Germany. *Proceedings of the National Academy of Sciences of the United States of America* 107: 19726–19730
- Wang XL, Wintle AG, Lu YC (2007) Testing a single-aliquot protocol for recuperated OSL dating. *Radiation Measurements* 42: 380–391
- Wintle AG (1973) Anomalous fading of thermo-luminescence in mineral samples. *Nature* 245: 143–144 ■